



Article

# Development and Performance Evaluation of Solid-Free Drilling Fluid for CBM Reservoir Drilling in Central Hunan

Pinghe Sun <sup>1,2</sup> , Meng Han <sup>1,2</sup> , Han Cao <sup>1,2,\*</sup>, Weisheng Liu <sup>1,2</sup>, Shaohe Zhang <sup>1,2</sup> and Junyi Zhu <sup>1,2</sup>

<sup>1</sup> Key Laboratory of Metallogenic Prediction of Nonferrous Metals and Geological Environment Monitoring, Ministry of Education, Changsha 410083, China; pinghesun@csu.edu.cn (P.S.); hanmeng@csu.edu.cn (M.H.); weishengliu@csu.edu.cn (W.L.); zhangshaohe@163.com (S.Z.); zhujunyi@csu.edu.cn (J.Z.)

<sup>2</sup> School of Geosciences and Info-Physics, Central South University, Changsha 410083, China

\* Correspondence: hancock@csu.edu.cn

Received: 9 August 2020; Accepted: 15 September 2020; Published: 16 September 2020



**Abstract:** Solid-free drilling fluid is a matter of cardinal significance in the course of Coal bed Methane (CBM) reservoir drilling. This study evaluated the performance of solid-free CBM drilling fluid in central Hunan. Three types of surfactants, namely TX-10 (nonionic), HSB1618 (zwitterionic) and penetrant T (anionic), were added in basic fluid at various concentrations of 0.05, 0.10 and 0.15% (m/m). This study comprised of drilling fluid rheology, sample mineral analysis, sample nuclear magnetic resonance (NMR) scanning, sample wettability, and sample surface micro characteristics tests. The results show that TX-10 and HSB1618 enhance the rheological properties of drilling fluid, such as yield point and gel strength. Penetrant T has opposite effect on it. It was found that the minimum American Petroleum Institute (API) filtration is only 0.3 mL. This study adopted a new method using laser particle size analyzer to evaluate suspension performance. Based on the surface micro characteristics of the sample and the NMR scanning tests, it is found that the residual amount of basic fluid + HSB1618 in the sample is the smallest. The wettability modification curve indicates that three surfactants decrease the sample's hydrophobicity. With the increase of surfactant concentration, all above parameters change regularly. The basic fluid + 0.10% HSB1618 has the strongest hydrophobicity for sample at pH = 10. This study obtained a set of solid-free drilling fluid system, which provides better suspension capacity and large contact angle and reduces residue of drilling fluid in CBM reservoir. Ultimately, it can accelerate the desorption of coal gas and reduce damage to the reservoir.

**Keywords:** CBM; surfactant; solid-free drilling fluid; CBM reservoir wettability

## 1. Introduction

Compared with conventional oil and natural gas, Coal bed Methane (CBM) is a kind of highly efficient and clean energy which has obvious advantages in safety, economy and environmental protection [1,2]. China is rich in CBM reserves, although having less than Russia and Canada. However, due to the complex geological conditions of domestic CBM reservoirs and development technology is somewhat behind, China's CBM exploration and development is still in the initial stage [3–6]. The deep layer in the middle Hunan area is dominated by conventional natural gas exploration, but the development of CBM plays an important role in the shallow gas development [7–9].

In CBM development, it is very important to use proper drilling fluid system for safe, efficient and environmental protection drilling. First of all, solid phase particles in drilling fluid tend to block the fractures and pores of the CBM reservoir, and then block the gas production channel. To reduce the

intrusion of solid phase particles into CBM reservoir, it is advisable to drill with solid-free drilling fluid with good suspension performance [10–12]. It has the characteristics of low density, good suspension performance and small filtration and maximize the control of solid intrusion which can reduce reservoir leakage and damage and is a perfect for low density drilling fluid system [13–15]. Secondly, the reservoir is easy to absorb or adsorb liquids and gases. When drilling fluid invasions into CBM reservoir, it is easy to change its surface wettability, thus affecting the desorption and percolation of CBM, and thereby affecting CBM productivity [16–20].

Foam drilling fluid has a special network structure, which can carry cuttings well. Cai et al. [21] improved the foaming volume of foamed drilling fluid up to 50% by using chemically treated nano-SiO<sub>2</sub> dispersions. By studying the foam's properties, Su et al. [22] found that the appropriate temperature was 40–100 °C and that the foaming performance of hard foam could maintain within 120 °C. Fractures and minerals affect the permeability of CBM reservoirs [23–28]. Cui et al. [29] combined FESEM with X-ray mu-CT together with EDS to quantify the mineral and fracture characteristics. Coal reservoir characteristics may be related to coal rank and maceral as well as mineral content [30]. Yang et al. [31] used NMR tests and got the scattergram of coal pore size at a variety of strain rates. It was found that the crest value in the fractures rose and the crest value for the meso-macropores declined with the fortify of strain rates. The T2 spectrum obtained by NMR can be converted to the pore throat distribution. Adebayo et al. [32] mentioned T2 is connected with the surface relaxivity and the pores surface to volume ratio.

Huang et al. [33] mentioned that SWIA could adjust the core wettability. Li et al. [34] and Shen et al. [35] mentioned that the surfactant can increase the wettability of coal, and further enhance the desorption of methane; it can advance the recovery factor in theory and critical desorption pressure of CBM. Drilling fluid and coal surface contact, its pH value directly affects the wettability, further influencing the permeability of CBM. Through a lot of experiments to study the influence of drilling fluid pH value on the coal wettability, Zheng et al. [36] found that wettability and drilling fluid pH value is related, first reduced, then increased, and finally reduced. The above research results have played an important role in accelerating the development of CBM drilling fluid. However, there is a lack of special evaluation on the rheological, wettability of drilling fluid and the amount of additives for the practical characteristics of CBM drilling, and the relevant research lacks a systematic approach and depth.

Therefore, this study takes this as the starting point to analyze the rock-carrying capacity of the solid-free drilling fluid and study the influence of surfactant concentration and pH in the solid-free drilling fluid on the wettability of the CBM reservoir in central Hunan. This study optimizes the indoor evaluation method of the suspension performance of the solid-free drilling fluid, optimizes the formulation of the solid-free drilling fluid for the central Hunan CBM reservoir, and reveals the wettability mechanism of the central Hunan CBM reservoir when the solid-free drilling fluid penetrates. It is of great significance to optimize the formulation of the solid-free drilling fluid during the development of CBM in central Hunan, which further contributes to the rational development of CBM resources and the improvement of CBM productivity in central Hunan.

## 2. Experimental Method

### 2.1. Materials

#### 2.1.1. CBM Reservoir Sample

The reserves of CBM resources are 2.8 billion m<sup>3</sup> and the abundance of resource reserves is 0.43 m<sup>3</sup>/km<sup>2</sup> in the Lengshuijiang mining area in central Hunan. The development prospect is broad. CBM reservoir sample of Lengshuijiang mining area was selected and made into  $\varnothing 20$  mm  $\times$  10 mm standard sample which has the same bedding direction and similar structure. Rock powder was obtained by crushing some samples and passing a 200-mesh sieve.

### 2.1.2. Surfactant

The mass fraction of nonionic surfactant TX-10 is 99%, which formed by condensation of nonylphenol and ethylene oxide in the presence of a catalyst. Its molecular formula is  $C_{15}H_{24}O \cdot (C_2H_4O)_n$ , where when  $n$  changes, the product has different properties and different applications. Its melting point is 44–46 °C, boiling point is 250 °C, density is 1.06 g/mL, and flash point is 535 °F. It does not exist in an ionic state in water and has good stability, which is not easy to be affected by strong electrolyte, acid and alkali. At the same time, good compatibility with other surfactants. The mass fraction of zwitterionic surfactant HSB1618 is 40% which has both ionic properties and excellent resistance to calcium and magnesium ions. Its free amine content is  $\leq 2\%$ , sodium chloride content is  $\leq 7\%$ , and organochlorine content is 0. The mass fraction of anionic surfactant penetrant T is 40% which is cheap and not resistant to strong acids and bases, reductants and metal salts. The pH value of 1% aqueous solution is 7.0–9.5. It works best when the temperature is less than 40 °C and the pH value is 5–10. Its active part tends to dissociate into negative ions in water, and there is a large organic anion that can interact with alkali to form salt.

### 2.2. Solid-Free Drilling Fluid

On the basis of previous research, the basic fluid of the solid-free drilling fluid was obtained as Table 1.

**Table 1.** The basic fluid composition.

Components	KCl	Na <sub>2</sub> CO <sub>3</sub>	XC	PAC
The mass fraction	3%	0.1%	0.2%	0.15%
Function	Inhibitor	Alkalinity regulator	Viscosities Foam stabilizer	Filtration loss reducer, Inhibitor

### 2.3. XRD

X-ray diffraction tests were carried out on reservoir samples in accordance with the SY/T5163–2010, and quantitative analysis of mineral composition was conducted using D8 Advance x-ray diffractometer of Bruker Company in Bremen, Germany. The contents of hard and brittle minerals and clay minerals were determined to study the microscopic mechanisms affecting the adsorption properties and wettability of samples.

### 2.4. Rheological Properties Test

The rheological properties test was conducted according to API standards. The time required to flow up to 500 mL of drilling fluid was measured by the funnel viscometer produced by Qingdao Tongchun Petroleum Instrument Co., Ltd. (QTPI) (Qingdao, China), which is the viscosity of drilling fluid (FV).

The ZNN-SD6 rotary viscometer produced by QTPI was used to obtain the drilling fluid viscosity and shear stress. The drilling fluid was placed in a circular space between two concentric cylinders. The outer cylinder rotates at a constant speed through variable transmission, and the outer cylinder produces a torque through the action of the measured drilling fluid on the inner cylinder, which makes the inner cylinder connected with the torsion spring rotate at a corresponding angle. According to Newton's law, the size of the angle is proportional to the viscosity of the drilling fluid, so the measurement of the viscosity turns to the measurement of the inner cylinder angle. By the sensor display value, readings at the different rpm values, i.e., 600, 300, 200, 100, 6 and 3 were measured, including gel strengths. The apparent viscosity (AV), yield point (YP) and plastic viscosity (PV) can be obtained by Equations (1)–(3).

$$AV = 0.5\varphi_{600} \quad (1)$$

$$PV = \varphi_{600} - \varphi_{300} \quad (2)$$

$$YP = 0.511(2\varphi_{300} - \varphi_{600}) \quad (3)$$

where  $\varphi_{600}$  is a 600-rpm dial reading of the viscometer;  $\varphi_{300}$  is a 300-rpm dial reading of the viscometer.

### 2.5. Filtration Test

According to the API standard, the filtration test was conducted using the ZNS-5A medium pressure filter press assembly produced by QTPI. First, 500 mL drilling fluid was injected into the cylindrical drilling fluid cup and the lid was tightened; then, the air source was connected to adjust the pressure to 0.69 MPa; and finally, the air valve was opened to let the air source enter the drilling fluid cup. The filtration area of the instrument was  $45.60 \pm 0.60 \text{ cm}^2$  ( $1 \pm 0.1 \text{ in}^2$ ). The time of filtration and the amount of filtration ( $F_{\text{API}}$ ) after filtration were measured. Meanwhile, the quality of filter cake was observed to measure the effect of borehole wall protection.

### 2.6. Laser Particle Size Analysis Test

Added 2 g of rock powder over 200 mesh sieve into 200 g solid-free drilling fluid, then stirred for 5 min and stood for 30 min, and extracted 20 mL of upper liquid. Distilled water was selected as the dispersion medium, and the particle size distribution of suspended rock powder in the liquid was analyzed by Rise-2002 laser particle size analyzer produced by Jinan Rise Science & Technology Co., Ltd. (Jinan, China), so as to further evaluate the suspension performance of the solid-free drilling fluid.

### 2.7. Wettability Test

Different solid-free drilling fluids were configured by varying the surfactant concentration and drilling fluid pH. The samples were soaked in different drilling fluids for 48 h and dried naturally for 24 h. JCY series contact angle instrument produced by Shanghai Fangrui Instrument Co., Ltd. (Shanghai, China) was used to measure the dynamic contact angle of distilled water on the samples within 0~12 s and obtain the contact angle photos. Then, the wetting modification effect of the solid-free drilling fluid on the samples was analyzed by comparing with the samples that were not soaked or soaked in water.

### 2.8. Microscope Test

The soaked sample was naturally dried for 24 h, and the adsorption state of drilling fluid on the sample surface was observed with SQ500MF high-power integrated video microscope produced by Shanghai victory & Shuangquan tech. (Shanghai, China). The magnification factor is 100, and the distribution state of different drilling fluids on the sample surface was observed by comparing with the sample soaked in water to further analyze the adsorption principle.

### 2.9. NMR Scanning Test

The soaked sample was wrapped in PTFE tape to reduce water evaporation. NMR scanning with MacroMR12-150H-I NMR scanner produced by Suzhou Niumag Analytical Instrument Corporation was used to obtain  $T_2$  spectrum and signal imaging. The  $T_2$  spectrum was converted into the pore size distribution to compare the pore size distribution of each sample under the saturated state.

According to the basic principle of NMR scanning imaging, the relaxation characteristics of fluid in porous media can be expressed by Equation (4). According to Equation (4), the relaxation time of NMR  $T_2$  is in direct proportion to the pore size ( $D = 2r$ ). If  $C = 2F_s\rho_2$ , the Equation (5) can be obtained. The  $T_2$  spectrum of rock can be converted into pore size distribution curve by Equation (5).

$$\frac{1}{T_2} \approx \rho_2 \frac{s}{v} = F_s \frac{\rho_2}{r} \quad (4)$$



$$D = CT_2 \quad (5)$$

where  $T_2$  is NMR transverse relaxation time, ms;  $\rho_2$  is rock transverse surface relaxation strength coefficient, nm/ms;  $S$  is total pore surface area of rock,  $\text{nm}^2$ ;  $V$  is pore volume of rock,  $\text{nm}^3$ ;  $r$  is pore radius, nm;  $F_s$  is geometric shape factor (spherical pores,  $F_s = 3$ ; Cylindrical pores,  $F_s = 2$ );  $D$  is pore diameter of the rock, nm;  $C$  is rock conversion coefficient, nm/ms.

### 3. Results and Discussions

#### 3.1. Mineral Analysis

XRD test results of samples are shown in Figure 1. The results show that the mineral content in the sample is 25% montmorillonite, 20% pyrophyllite, 16% illite, 13% quartz, 12% kaolin, 11% pyrite and 3% anatase. Clay minerals are mainly montmorillonite and illite with content up to 53.

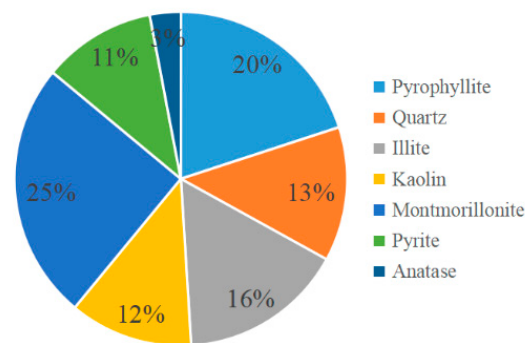


Figure 1. The mineral analysis of coal bed methane (CBM) reservoir sample.

#### 3.2. Statistical Analysis of Rheological Properties

The rheological parameters of the solid-free drilling fluid with different concentrations of TX-10, HSB1618 and penetrant T are shown in Table 2. The apparent viscosity of basic fluid + HSB1618 is the largest, indicating the maximum consistency. When the surfactant concentration is 0.10%, the API filtration of basic fluid + HSB1618 is also the minimum. On the contrary, the apparent viscosity of basic fluid + penetrant T is the smallest, the filtration is the largest, and the performance parameters of basic fluid + TX-10 are in the middle. The funnel viscosity and apparent viscosity of several drilling fluids have the same rule. No matter what kind of surfactant is added, the API filtration is small and the filter cake is thin and tough, which is an ideal drilling fluid parameter and has good wall protection effect.

Table 2. The rheological properties of solid-free drilling fluid.

Drilling Fluid	Basic Fluid + TX-10			Basic Fluid + HSB1618			Basic Fluid + Penetrant T		
	0.05	0.10	0.15	0.05	0.10	0.15	0.05	0.10	0.15
$C_{\text{Surfactant}}/\%$									
FV/s	22	24	36	25	35	42	21	18	17
$F_{\text{API}}/\text{mL}$	2.2	1.9	1.8	2.6	0.8	0.3	0.8	3.0	5.2
AV/MPa·s	9.8	14.8	14.9	11.2	14.7	16.2	8.9	5.9	5.7
PV/MPa·s	6.4	10.2	10.1	7.9	9.1	9.3	5.8	4.2	3.6
YP/Pa	3.44	4.61	4.95	3.41	5.76	7.04	3.21	1.81	2.07
pH	9.0	9.0	9.0	9.5	9.5	9.5	8.5	8.5	8.5
$\rho/\text{g}\cdot\text{cm}^{-3}$	0.87	0.80	0.77	0.81	0.78	0.75	1.0	1.0	1.0

The horizontal displacement of CBM reservoir is long, and cuttings are not easy to be carried during drilling, so the rheological property of drilling fluid should be adjusted to make it have good suspension and rock carrying capacity. The yield point of the solid-free drilling fluid with different concentrations of surfactants is shown in Figure 2. As can be seen from the figure, the yield point

of basic fluid + penetrant T is very small, while basic fluid + HSB1618 and basic fluid + TX-10 have higher yield point. The difference increases with the concentration of surfactant and is very small when the concentration is 0.05%. As the concentration of surfactant increases, the yield point of basic fluid + HSB1618 and basic fluid + TX-10 increases, while basic fluid + penetrant T has an obvious downward trend. In conclusion, the results show that the basal fluid + HSB1618 has higher yield point, better rock-carrying and hole-cleaning capacity.

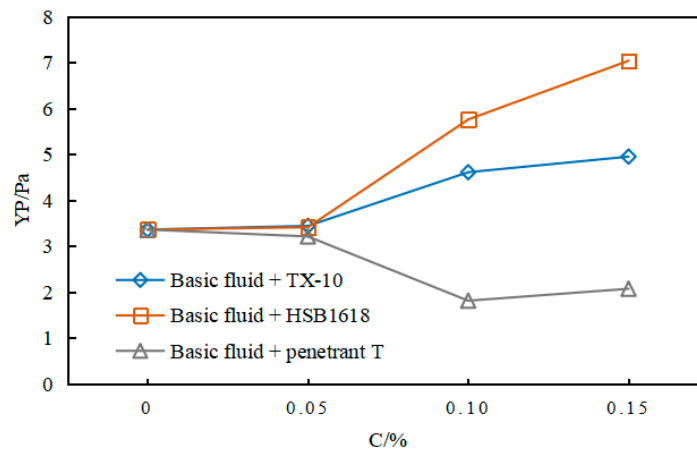


Figure 2. The yield point of solid-free drilling fluid.

The gel strengths of the solid-free drilling fluid with different concentrations of surfactants is shown in Figure 3. It can be seen from the figure that when the concentration of surfactant is 0.10% and 0.15%, the gel 10 min and the gel 10 sec of basic fluid + TX-10 and basic fluid + HSB1618 have sufficient range, while the gel strengths of basic fluid + penetrant T is very small, and the difference between the gel 10 min and the gel 10 sec is very small. With the increase of surfactant concentration, the gel strengths of basic fluid + TX-10 and basic fluid + HSB1618 increased, while that of basic fluid + penetrant T decreased. At the concentration of 0.05%, the gel strengths of basic fluid + HSB1618 is less than that of basic fluid + TX-10. With the increase of the concentration, the gel strengths of basic fluid + HSB1618 is gradually greater than that of basic fluid + TX-10. The results show that the basic fluid + TX-10 and the basic fluid + HSB1618 have good suspension performance at the surfactant concentration of 0.10% and 0.15%, which can effectively reduce the formation of cuttings bed in the horizontal section of CBM reservoir drilling.

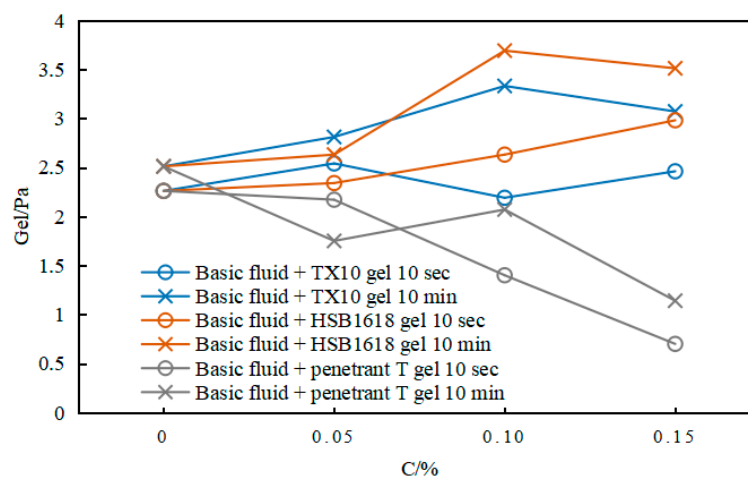
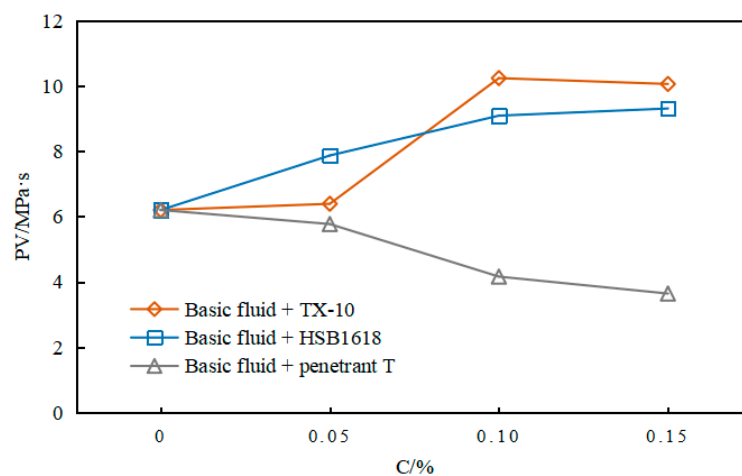


Figure 3. The gel strength of solid-free drilling fluid.

The plastic viscosity of the solid-free drilling fluid with different concentrations of surfactants is shown in Figure 4. The plastic viscosity reflects the internal friction between suspended particles and liquid phase as well as continuous liquid phase in the dynamic equilibrium of the destruction and recovery of network structure in drilling fluid under laminar flow. The main factor affecting the plastic viscosity is the content of solid phase, the higher the content of solid phase, the greater the plastic viscosity. In addition, clay dispersion and polymer viscosifier also have an impact on the plastic viscosity, because they can affect the volume fraction or liquid viscosity. In these drilling fluids, basic fluid + TX-10 and basic fluid + HSB1618 have higher plastic viscosities than basic fluid + penetrant T. Surfactants TX-10 and HSB1618 act as viscosifier in drilling fluids, and penetrant T acts as viscosity reducers. With the increase of surfactant concentration, the plastic viscosity of the basic fluid + TX-10 and the basic fluid + HSB1618 increases, and the basic fluid + penetrant T decreases. The change of surfactant and its concentration change the plastic viscosity of drilling fluid by changing the liquid viscosity.



**Figure 4.** The plastic viscosity of solid-free drilling fluid.

### 3.3. Micro Analysis of Drilling Fluid Suspension Performance

According to the experimental data of laser particle size analysis, the particle size ranges of basic fluid + TX-10, basic fluid + HSB1618 and basic fluid + penetrant T are 22.664–637.059  $\mu\text{m}$ , 29.703–1118.3  $\mu\text{m}$  and 0.049–2.603  $\mu\text{m}$ , respectively. Basic fluid + HSB1618 suspended rock powder has the largest particle size, followed by basic fluid + TX-10, and basic fluid + penetrant T is the smallest. The particle size of the first 20 differentials is select to draw a graph, and the particle size analysis of the suspended rock powder in the solid-free drilling fluid is shown in Figure 5. With the increase of surfactant concentration, the differentials of rock powder suspended by basic fluid + TX-10 and basic fluid + HSB1618 increases, while the basic fluid + penetrant T does not change much. The maximum differential particle size of basic fluid + 0.15% TX-10, basic fluid + 0.15% HSB1618 and basic fluid + 0.15% penetrant T suspension is 164.744, 309.681 and 0.327  $\mu\text{m}$ , respectively. The maximum differential particle size of basic fluid + 0.05% HSB1618, basic fluid + 0.10% HSB1618 and basic fluid + 0.15% HSB1618 are 150.539, 258.582, 309.681  $\mu\text{m}$ , respectively. Basic fluid + HSB1618 has better suspension capacity, firstly because of its large consistency and gel strengths, and secondly because of the ionization of carboxyl, phenolic hydroxyl group and other functional groups on the rock powder surface, which makes the surface negatively charged. The compression of the double electric layer increases the electrostatic repulsion after HSB1618 is added, which is beneficial to the suspension of rock powder.

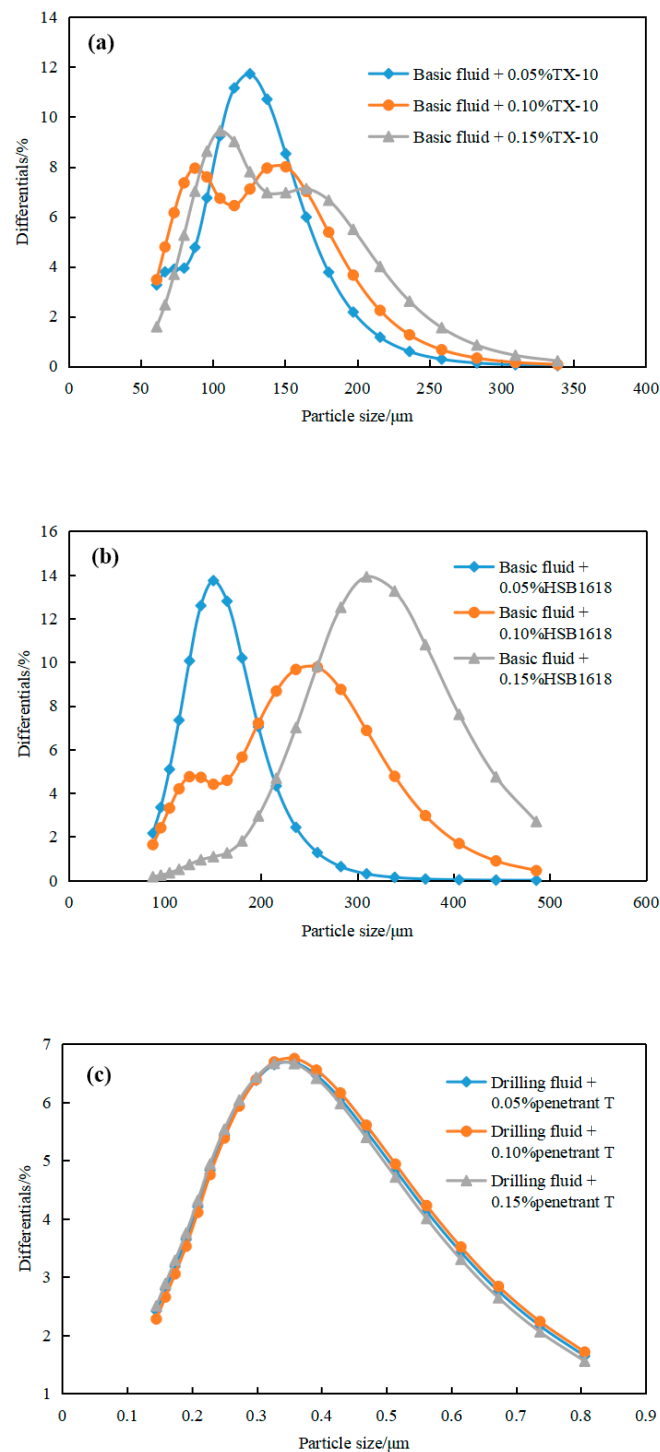


**Figure 5.** The particle size of the suspended rock powder in (a) basic fluid + TX-10, (b) basic fluid + HSB1618 and (c) basic fluid + penetrant T.

### 3.4. Adsorption Mechanism of Drilling Fluid

Drilling fluid with 0.10% (a) TX-10, (b) HSB1618, (c) penetrant T added to the basic fluid is shown in Figure 6. It can be seen from the figure that, when the concentration of surfactant is 0.10%, basic fluid + TX-10 and basic fluid + HSB1618 are rich in foam, while basic fluid + penetrant T has poor foamability. The foaming volume of the 200 mL of drilling fluid is 250, 240 and 200 mL, respectively. The basic fluid + TX-10 foam is loose while the basic fluid + HSB1618 foam is fine and uniform.



**Figure 6.** The basic fluid is added with 0.10% (a) TX-10, (b) HSB1618 and (c) penetrant T.

CBM reservoirs are highly absorbent which can absorb various liquids and gases. After different drilling fluids (a) water, (b) basic fluid + 0.10%TX-10, (c) basic fluid + 0.10%HSB1618, (d) basic fluid + 0.10%penetrant T, the microscopic diagram of sample surface is shown in Figure 7. According to the figure, there is no significant change on the sample surface after soaking in water, and fracture can be clearly seen on the surface. The basic fluid + 0.10% TX-10 is block or strip on the sample surface with uneven distribution. The basic fluid + 0.10%HSB1618 is evenly spread on the surface of sample, showing a thin layer, while the basic fluid + 0.10%penetrant T has a small adsorption capacity on the sample surface, and is distributed in a granular or strip form with uneven distribution. In the dense adsorption layer of basic fluid + 0.10%HSB1618, the hydrophilic group of HSB1618 points to the aqueous phase, and the sample surface is changed from hydrophobic to hydrophilic.

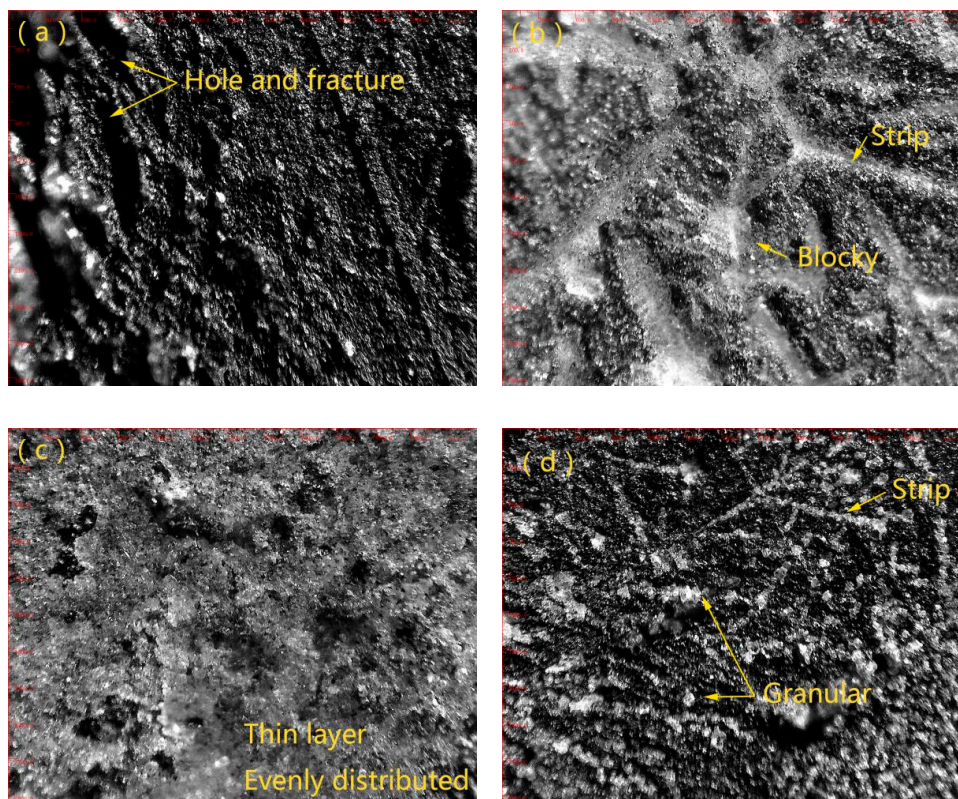


**Figure 7.** The microscopic photos of sample surface soaked by different drilling fluids: (a) water, (b) basic fluid + 0.10% TX-10, (c) basic fluid + 0.10%HSB1618 and (d) basic fluid + 0.10 penetrant T.

Penetrant T is an anionic surfactant with negative charge, while the carboxyl and phenolic hydroxyl group on the CBM reservoir surface ionizes, making the sample surface also negatively charged. The adsorption capacity of anionic surfactant on CBM reservoir surface is minimal due to electrostatic interaction. HSB1618 is a zwitterionic surfactant consisting of anionic and cationic surfactants, in which the cationic part is adsorbed by electrostatic interaction. TX-10 is a nonionic



surfactant that has no charge and cannot be adsorbed on the sample surface by electrostatic interaction. However, the hydrophobic non-polar groups such as aliphatic hydrocarbon and aromatic hydrocarbon on the sample surface make it hydrophobic. The main forces between nonionic surfactant and sample surface are hydrophobic and dispersive forces. In the case of minimal adsorption of penetrant T, basic fluid + penetrant T has better wetting effect, because penetrant T has high permeability, fast and uniform permeability, which can quickly fill pores on the sample surface to play a wetting role.

### 3.5. Application of NMR Pore Throat Distribution Curve

The NMR T2 spectrum of each sample obtained by MRI scanning was converted into pore throat distribution, as shown in Figure 8. The pore throats of the samples are concentrated in the interval 0.01~0.1  $\mu\text{m}$ , and the curves presented a bimodal shape, with the right peak being lower, that is, the proportion of large pore throats is small.

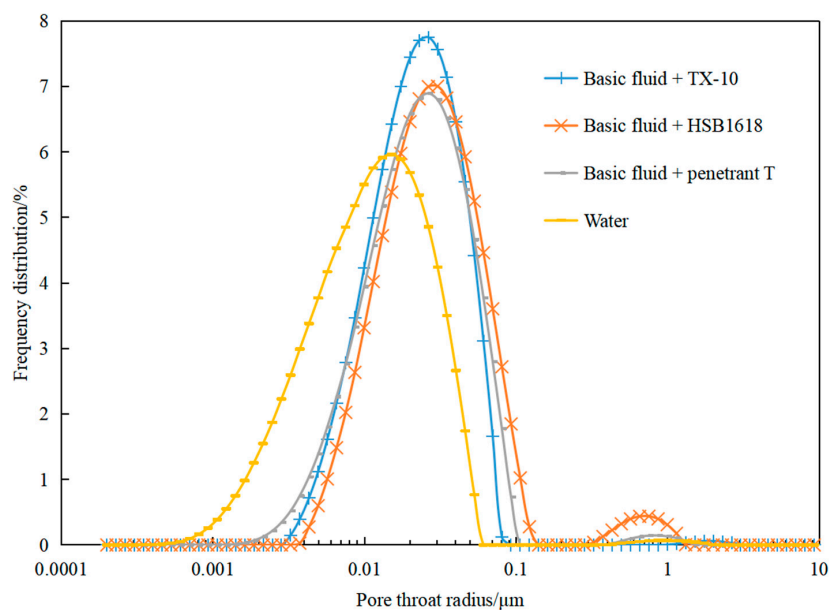


**Figure 8.** Pore throat distribution of samples soaked by different drilling fluids.

By comparing the distribution of NMR pore throat of samples soaked by different drilling fluids, it is found that the average pore throat of samples soaked by drilling fluids is greater than that of samples soaked by water. As the surfactant in the drilling fluid is hydrophilic, the pore fluid of samples soaked in the drilling fluid is larger than that soaked in water, resulting in a slightly larger pore throat radius. The pore throat frequency distribution of the sample soaked by basic fluid + TX-10 is the highest, and the 0.026- $\mu\text{m}$  pore throat frequency distribution reaches the highest, 7.7%. The hydrophilicity of different surfactants is different, and the pore throat distribution of the samples soaked by three kinds of drilling fluid is different. This difference is also related to the difference in drilling fluid NMR results and samples.

### 3.6. Transverse and Longitudinal Section Imaging

NMR scan imaging of samples soaked by different drilling fluids is shown in Figure 9. In terms of adsorption degree and residual amount, the cross-sectional imaging showed that the more red parts, the more liquid. The adsorption degree and residual amount in the sample ranged from large to small as basic fluid + TX-10, water, basic fluid + penetrant T and basic fluid + HSB1618. During immersion, the samples were placed longitudinally. In terms of saturation changes at different longitudinal positions, the cross-sectional imaging showed that the longitudinal saturation change from large to small was basic fluid + TX-10, basic fluid + penetrant T, basic fluid + HSB1618 and the water.

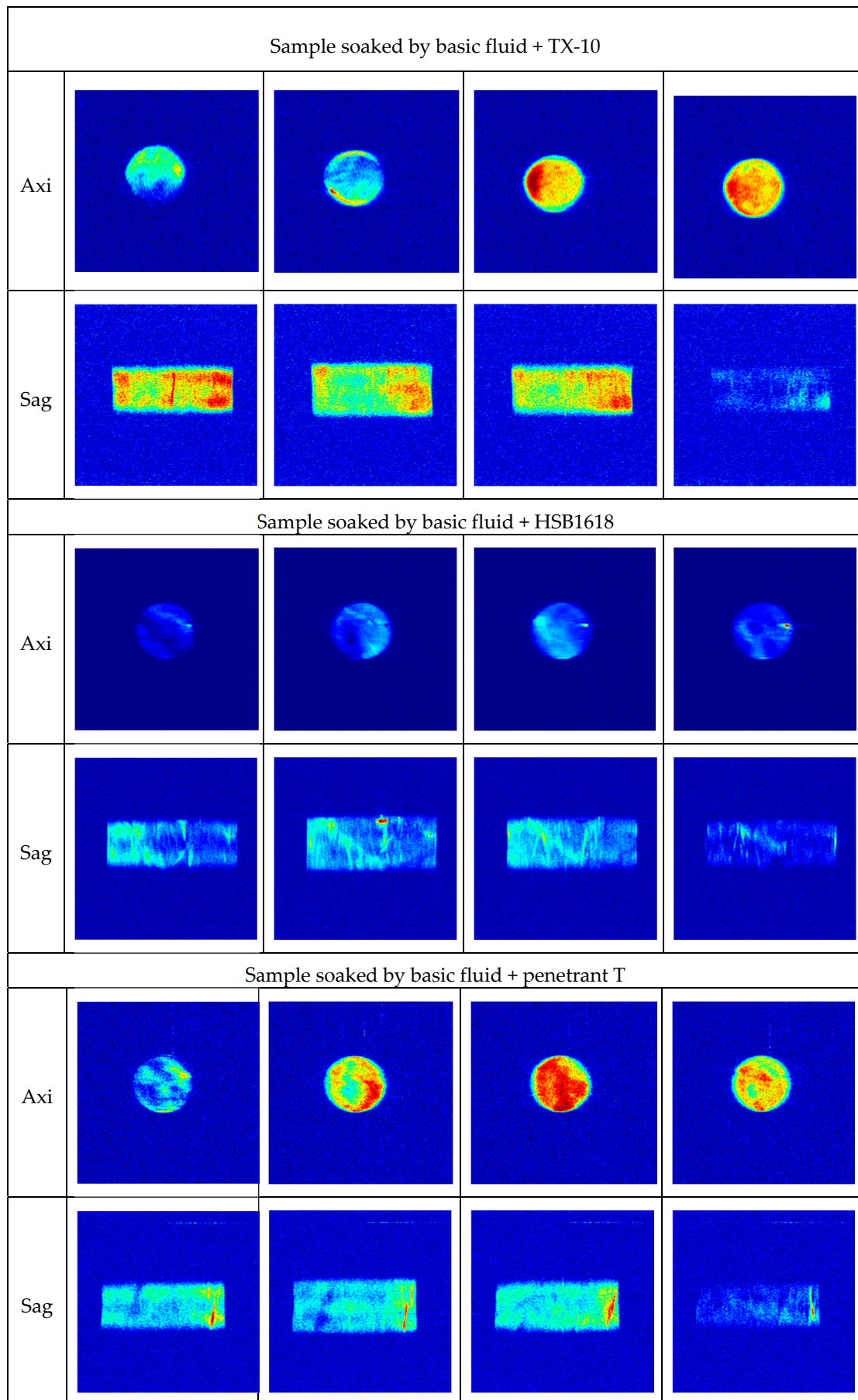


Figure 9. Cont.



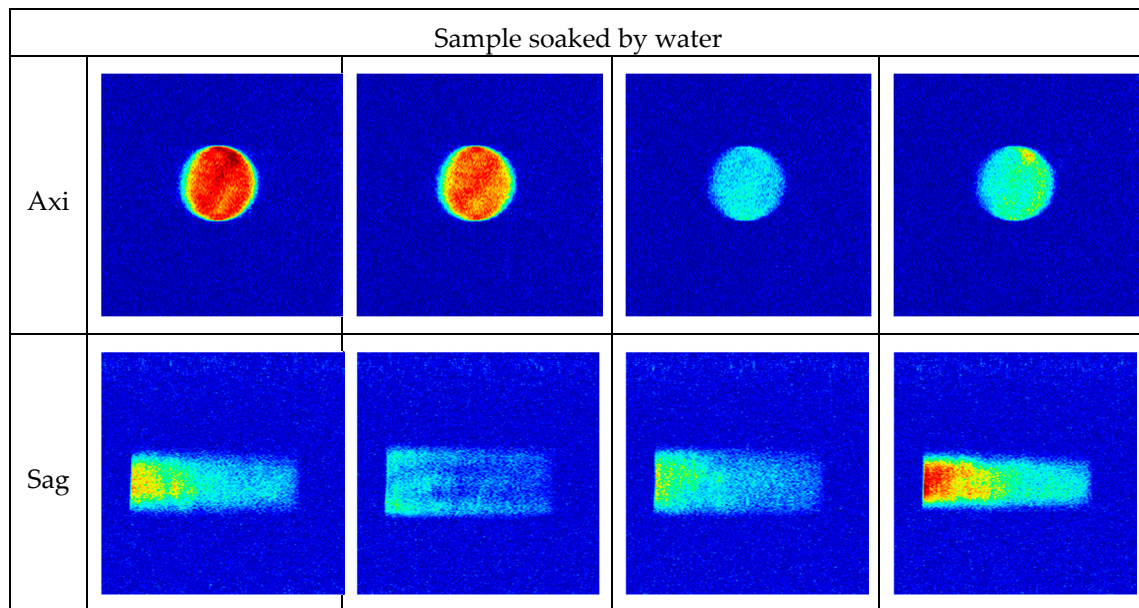


Figure 9. NMR imaging of samples soaked by different drilling fluids.

The basic fluid + HSB1618 should be selected based on the comprehensive comparison of adsorption degree, residual amount and saturation changes at different positions in the longitudinal direction. At the same time, because of the strong heterogeneity of samples, the difference of each sample has an impact on the results. In the drilling process of CBM reservoir in Central Hunan, 3%KCl + 0.1%Na<sub>2</sub>CO<sub>3</sub> + 0.1%HSB1618 + 0.2%XC + 0.1%PAC can reduce the residual drilling fluid in CBM reservoir and further reduce the damage to the reservoir.

### 3.7. Effect of Solid-Free Drilling Fluid Additive on Wettability of CBM Reservoir

The dynamic and static contact angles of the solid-free drilling fluid to the sample are shown in Figures 10 and 11. It can be seen from the figure that the contact angle of the unsoaked sample is the largest and does not change with time. The contact angle changes very little after water soaking, which indicates that the wettability of water to sample is very weak. The contact angle of sample decreases after soaked in three kinds of solid-free drilling fluids, and the trend of dynamic contact angle decrease significantly, indicating that the three kinds of drilling fluids can greatly increase the moisture of sample. The wetting ability of drilling fluid added with 0.10% surfactant is different to some extent. The wetting ability of drilling fluid added with 0.10% surfactant is as follows: basic fluid + penetrant T, basic fluid + HSB1618 and basic fluid + TX-10.

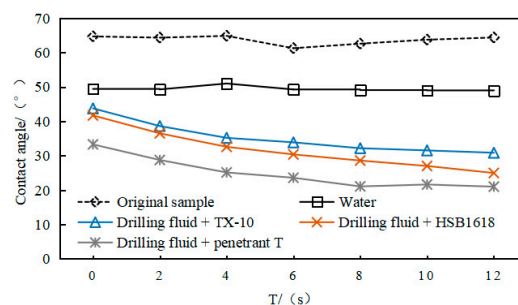
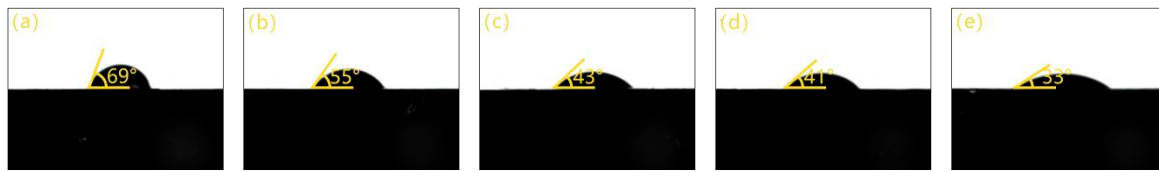
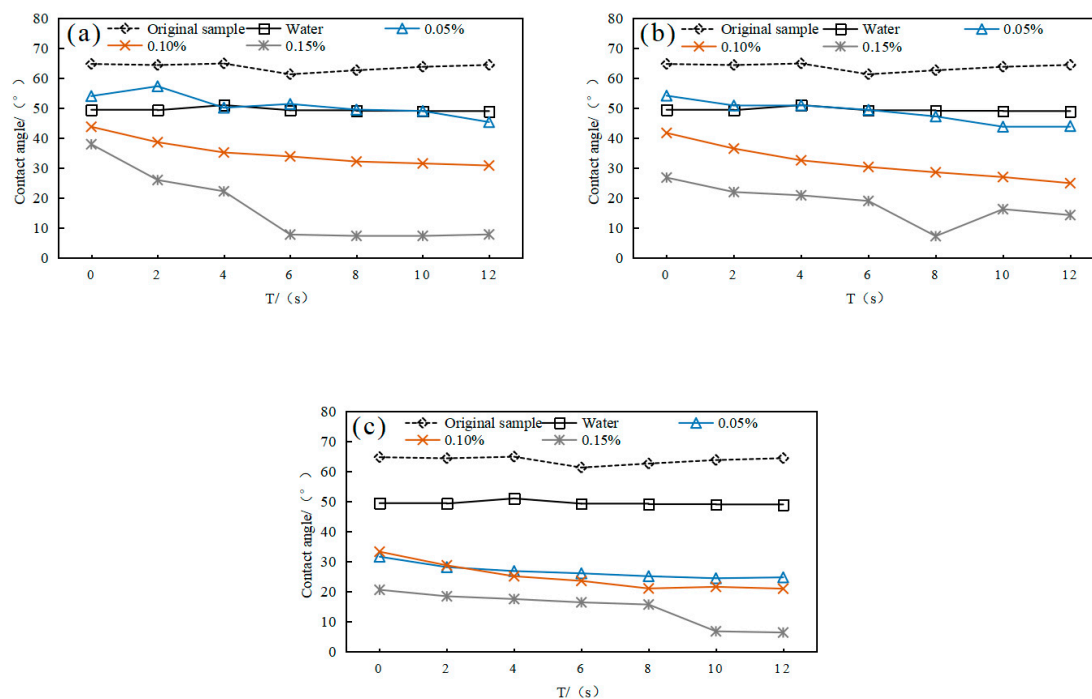


Figure 10. The contact angle variation of solid-free drilling fluid to sample.



**Figure 11.** The contact angle of (a) original sample and sample soaked by different drilling fluids (b) water, (c) basic fluid + 0.10% TX-10, (d) basic fluid + 0.10% HSB1618 and (e) basic fluid + 0.10% penetrant T.

The curve of contact angle of sample with different concentrations (a) TX-10, (b) HSB1618 and (c) penetrant T added to the basic fluid is shown in Figure 12. According to the figure, with the increase of surfactant concentration, the wettability of the three drilling fluids to sample increases to different degrees, in which the wettability of basic fluid + TX-10 and basic fluid + HSB1618 increases significantly. The wettability of basic fluid + 0.05% TX-10 and basic fluid + 0.05% HSB1618 is similar to that of water, while basic fluid + 0.05% penetrant T can significantly increase the wettability of sample. When the surfactant concentration is 0.15%, the dynamic contact angle of the three drilling fluids fluctuates greatly, which greatly improves the moisture of the sample.



**Figure 12.** The contact angle variation of different concentrations (a) TX-10, (b) HSB1618 and (c) penetrant T added in basic fluid to sample.

### 3.8. Effect of Solid-Free Drilling Fluid pH on Wettability of CBM Reservoir

According to the rheological properties and wetting effect of drilling fluid, HSB1618, the surfactant with the best effect, is selected and the pH of drilling fluid is changed at the optimal concentration of 0.10%. The change of contact angle of drilling fluid pH to sample is shown in Figure 13. It can be seen from the figure that the contact angle increases between pH 8–10, that is, the hydrophilicity of sample decreases. pH 10–12 shows a decreasing trend, that is, the hydrophilicity of sample increase. The contact angle is the smallest at pH 12, and the wetting effect of the drilling fluid on the sample is maximized. The contact angle is the largest at pH = 10, and the hydrophobicity of the drilling fluid to the sample is minimal. The change of hydrophilicity of sample is because the change of drilling

fluid pH affects the ionization degree of carboxyl and phenol hydroxyl group on sample surface, further changes the sample surface potential, and finally affects the wettability.

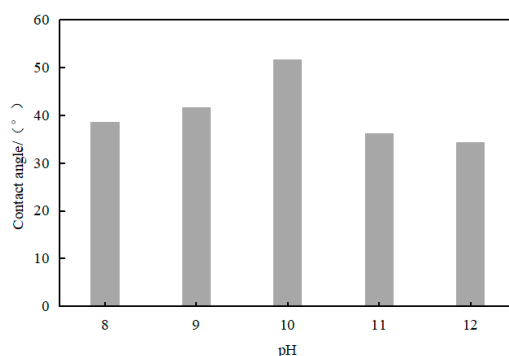


**Figure 13.** The contact angle variation of solid-free drilling fluid pH to sample.

#### 4. Conclusions

The performance of solid-free CBM drilling fluid in central Hunan have been examined. The results show that TX-10 and HSB1618 enhance the rheological properties of drilling fluid, such as yield point and gel strength. It was found that the minimum API filtration is only 0.3 mL. Experimental results show that the suspended cuttings capacity is successively from large to small: basic fluid + HSB1618, basic fluid + TX-10 and basic fluid + penetrant T in the drilling process of CBM reservoir in central Hunan. With the increase of surfactant concentration, the suspended cuttings capacity of basic fluid + HSB1618 and basic fluid + TX-10 increase. The residual amount of basic fluid + HSB1618 in the sample is the smallest. The longitudinal saturation changes from large to small was basic fluid + TX-10, basic fluid + penetrant T, basic fluid + HSB1618 and the water.

With the increase of surfactant concentration, the wettability of the three drilling fluids to samples increases in different degrees. When the surfactant concentration is 0.15%, the dynamic contact angle of the three drilling fluids fluctuates greatly, which greatly improves the water wettability of the samples. The basic fluid + permeant T has the best ability to improve the wettability of the reservoir surface in the drilling process of CBM reservoir in central Hunan. The hydrophilicity of samples decrease when the basic fluid + HSB1618 is at pH 8–10, while that of samples increase at pH 10–12.

In the process of CBM development in central Hunan, the solid-free drilling fluid formula 3%KCl + 0.1%Na<sub>2</sub>CO<sub>3</sub> + 0.1%HSB1618 + 0.2%XC + 0.1%PAC has strong suspension performance and large moistening contact angle, which is helpful for the flowback of drilling fluid, and can reduce the residual amount of drilling fluid in CBM reservoir, and finally reduce the damage to reservoir. Only three kinds of surfactants are discussed in this paper, and the application of cationic surfactants in solid-free drilling fluid can be studied in the future. In the follow-up studies, it is planned to carry out comparative studies of CBM reservoirs in multiple regions and study the acoustic and mechanical properties of reservoir samples before and after the action of solid-free drilling fluid.

**Author Contributions:** Conceptualization, P.S., M.H. and H.C.; Methodology, P.S., H.C. and S.Z.; Software, M.H. and J.Z.; Validation, P.S., W.L., M.H. and J.Z.; Writing—Original Draft Preparation, P.S., M.H., S.Z. and H.C.; Writing—Review and Editing, P.S., M.H., S.Z., W.L., and H.C. All authors have read and agreed to the published version of the manuscript.

**Funding:** This study was supported by Hunan Provincial Innovation Foundation for Postgraduate (No. 2019zzts162), the National Natural Science Foundation of China (No. 41602372), the open fund of the State Key Laboratory of Oil and Gas Reservoir Geology and Exploitation (Southwest Petroleum University, No. PLN201609 & No. PLN201607) and the fund of Ministry of Land and Resources Key Laboratory of Drilling Technology in Complex Conditions (No. DET201612).

**Acknowledgments:** All of the authors would like to direct their thanks to the professors and students in the Key Laboratory of Metallogenic Prediction of Nonferrous Metals and Geological Environment Monitoring (Central South University), Ministry of Education.

**Conflicts of Interest:** The authors declare no conflict of interest.

## References

- Golsanami, N.; Sun, J.; Liu, Y.; Yan, W.; Lianjun, C.; Jiang, L.; Dong, H.; Zong, C.; Wang, H. Distinguishing fractures from matrix pores based on the practical application of rock physics inversion and NMR data: A case study from an unconventional coal reservoir in China. *J. Nat. Gas Sci. Eng.* **2019**, *65*, 145–167. [[CrossRef](#)]
- Le, T.D.; Moyne, C.; Murad, M.A.; Panfilova, I. A three-scale poromechanical model for swelling porous media incorporating solvation forces: Application to enhanced coalbed methane recovery. *Mech. Mater.* **2019**, *131*, 47–60. [[CrossRef](#)]
- Zheng, M.; Li, J.; Wu, X.; Wang, S.; Guo, Q.; Yu, J.; Zheng, M.; Chen, N.; Yi, Q. China's conventional and unconventional natural gas resources: Potential and exploration targets. *J. Nat. Gas Geosci.* **2018**, *3*, 295–309. [[CrossRef](#)]
- Song, Y.; Ma, X.; Liu, S.; Jiang, L.; Hong, F.; Qin, Y. Accumulation conditions and key technologies for exploration and development of Qinshui coalbed methane field. *Pet. Res.* **2018**, *3*, 320–335. [[CrossRef](#)]
- Long, Q.; Hu, Q.; Zhang, Z.; Ren, T. On factors affecting coalbed gas content measurement. *Measurement* **2018**, *121*, 47–56. [[CrossRef](#)]
- Hao, C.; Cheng, Y.; Dong, J.; Liu, H.; Jiang, Z.; Tu, Q. Effect of silica sol on the sealing mechanism of a coalbed methane reservoir: New insights into enhancing the methane concentration and utilization rate. *J. Nat. Gas Sci. Eng.* **2018**, *56*, 51–61. [[CrossRef](#)]
- Wang, X.; Li, J.; Xu, S.; Lin, L.; Liu, Z.; Tan, H. Preliminary evaluation of hydraulic fracturing effects of coalbed methane wells in central Hunan. *China Coalbed Methane* **2018**, *15*, 3–8.
- Zhu, W.; Gu, S. Feasibility and risk analysis of coalbed methane development in central Hunan. *China Saf. Sci. J.* **2010**, *20*, 97–101.
- Yi, H. Study on characteristics of coalbed methane reservoirs in the lower carboniferous water measurement group in central Hunan. *Coal Geol. China* **2010**, *22*, 22–25.
- Xu, J.; Zhai, C.; Ranjith, P.G.; Sun, Y.; Qin, L. Petrological and ultrasonic velocity changes of coals caused by thermal cycling of liquid carbon dioxide in coalbed methane recovery. *Fuel* **2019**, *249*, 15–26. [[CrossRef](#)]
- Zheng, C.; Jiang, B.; Xue, S.; Chen, Z.; Li, H. Coalbed methane emissions and drainage methods in underground mining for mining safety and environmental benefits: A review. *Process. Saf. Environ. Prot.* **2019**, *127*, 103–124. [[CrossRef](#)]
- Liu, D.; Wang, Q.; Wang, Y.; Wang, H.; Yu, H.; Yuan, M. Laboratory research on degradable drilling-in fluid for complex structure wells in coalbed methane reservoirs. *Pet. Explor. Dev.* **2013**, *40*, 249–253. [[CrossRef](#)]
- Shi, Z.; Zhao, Y.; Qi, H.; Liu, J.; Hu, Z. Research and Application of Drilling Technology of Extended-reach Horizontally-intersected Well Used to Extract Coalbed Methane. *Procedia Earth Planet. Sci.* **2011**, *3*, 446–454. [[CrossRef](#)]
- Gentzis, T.; Deisman, N.; Chalaturnyk, R.J. Effect of drilling fluids on coal permeability: Impact on horizontal wellbore stability. *Int. J. Coal Geol.* **2009**, *78*, 177–191. [[CrossRef](#)]
- Rafati, R.; Smith, S.R.; Haddad, A.S.; Novara, R.; Hamidi, H. Effect of nanoparticles on the modifications of drilling fluids properties: A review of recent advances. *J. Pet. Sci. Eng.* **2018**, *161*, 61–76. [[CrossRef](#)]
- Chattaraj, S.; Mohanty, D.; Kumar, T.; Halder, G. Thermodynamics, kinetics and modeling of sorption behaviour of coalbed methane—A review. *J. Unconv. Oil Gas Resour.* **2016**, *16*, 14–33. [[CrossRef](#)]
- Xi, X.; Jiang, S.G.; Zhang, W.; Wang, K.; Shao, H.; Wu, Z. An experimental study on the effect of ionic liquids on the structure and wetting characteristics of coal. *Fuel* **2019**, *244*, 176–183. [[CrossRef](#)]
- Roussi, L.; Stihle, J.; Geantet, C.; Uzio, D.; Tayakout-Fayolle, M. Coal-derived liquid asphaltene diffusion and adsorption in supported hydrotreating catalysts. *Fuel* **2013**, *109*, 167–177. [[CrossRef](#)]
- Shaida, M.A.; Dutta, R.K.; Sen, A.K. Removal of diethyl phthalate via adsorption on mineral rich waste coal modified with chitosan. *J. Mol. Liq.* **2018**, *261*, 271–282. [[CrossRef](#)]
- Jawad, A.H.; Ismail, K.; Ishak, M.A.M.; Wilson, L.D. Conversion of Malaysian low-rank coal to mesoporous activated carbon: Structure characterization and adsorption properties. *Chin. J. Chem. Eng.* **2019**, *27*, 1716–1727. [[CrossRef](#)]

21. Cai, J.; Gu, S.; Wang, F.; Yang, X.; Yue, Y.; Wu, X.; Chixotkin, V.F. Decreasing Coalbed Methane Formation Damage Using Microfoamed Drilling Fluid Stabilized by Silica Nanoparticles. *J. Nanomater.* **2016**, *2016*, 1–11. [[CrossRef](#)]
22. Su, J.; Dong, W.; Zhou, S.; Deng, M. Synthesis and Assessment of a CO<sub>2</sub>-Switchable Foaming Agent Used in Drilling Fluids for Underbalanced Drilling. *J. Surfactants Deterg.* **2018**, *21*, 375–387. [[CrossRef](#)]
23. Zhu, H.; Tang, X.; Jiang, S.; Liu, S.; Zhang, B.; Jiang, S.; McLennan, J.D. Permeability stress-sensitivity in 4D flow-geomechanical coupling of Shouyang CBM reservoir, Qinshui Basin, China. *Fuel* **2018**, *232*, 817–832. [[CrossRef](#)]
24. Clarkson, C.R.; Salmachi, A. Rate-transient analysis of an undersaturated CBM reservoir in Australia: Accounting for effective permeability changes above and below desorption pressure. *J. Nat. Gas Sci. Eng.* **2017**, *40*, 51–60. [[CrossRef](#)]
25. Wang, Z.; Qin, Y. Physical experiments of CBM coproduction: A case study in Laochang district, Yunnan province, China. *Fuel* **2019**, *239*, 964–981. [[CrossRef](#)]
26. Akhondzadeh, H.; Keshavarz, A.; Sayyafzadeh, M.; Kalantariasl, A. Investigating the relative impact of key reservoir parameters on performance of coalbed methane reservoirs by an efficient statistical approach. *J. Nat. Gas Sci. Eng.* **2018**, *53*, 416–428. [[CrossRef](#)]
27. Ivakhnenko, O.P.; Makhatoeva, M.N.; Nadirov, K.; Bondarenko, V. Unconventional Coalbed Methane Reservoirs Characterization Using Magnetic Susceptibility. *Energy Procedia* **2016**, *97*, 318–325. [[CrossRef](#)]
28. Morad, K. Selected topics in coalbed methane reservoirs. *J. Nat. Gas Sci. Eng.* **2012**, *8*, 99–105. [[CrossRef](#)]
29. Cui, J.; Liu, D.; Cai, Y.; Pan, Z.; Zhou, Y. Insights into fractures and minerals in subbituminous and bituminous coals by FESEM-EDS and X-ray  $\mu$ -CT. *Fuel* **2019**, *237*, 977–988. [[CrossRef](#)]
30. Yuan, Y.; Tang, Y.; Shan, Y.; Zhang, J.; Cao, D.; Wang, A. Coalbed methane reservoir evaluation in the Manas mining area, southern Junggar Basin. *Energy Explor. Exploit.* **2018**, *36*, 114–131. [[CrossRef](#)]
31. Yang, Z.; Fan, C.; Lan, T.; Li, S.; Wang, G.; Luo, M.; Zhang, H. Dynamic Mechanical and Microstructural Properties of Outburst-Prone Coal Based on Compressive SHPB Tests. *Energies* **2019**, *12*, 4236. [[CrossRef](#)]
32. Adebayo, A.R.; Babalola, L.O.; Hussaini, S.R.; Alqubalee, A.; Babu, R.S. Insight into the Pore Characteristics of a Saudi Arabian Tight Gas Sand Reservoir. *Energies* **2019**, *12*, 4302. [[CrossRef](#)]
33. Huang, W.; Lei, M.; Qiu, Z.; Leong, Y.-K.; Zhong, H.; Zhang, S. Damage mechanism and protection measures of a coalbed methane reservoir in the Zhengzhuang block. *J. Nat. Gas Sci. Eng.* **2015**, *26*, 683–694. [[CrossRef](#)]
34. Li, P.; Ma, D.; Zhang, J.; Tang, X.; Huo, Z.; Li, Z.; Liu, J. Effect of Wettability on Adsorption and Desorption of Coalbed Methane: A Case Study from Low-Rank Coals in the Southwestern Ordos Basin, China. *Ind. Eng. Chem. Res.* **2018**, *57*, 12003–12015. [[CrossRef](#)]
35. Shen, J.; Zhao, J.; Qin, Y.; Shen, Y.; Wang, G.G. Water imbibition and drainage of high rank coals in Qinshui Basin, China. *Fuel* **2018**, *211*, 48–59. [[CrossRef](#)]
36. Zheng, S.; Huang, Z.; Yao, A. Research on the effect of drilling fluid's pH value on the coal's wettability. *J. Pet. Explor. Prod. Technol.* **2017**, *8*, 849–853. [[CrossRef](#)]

